In Situ Compatibilization Between Polystyrene-Grafted Nano-Sized TiO_2 and Polypropylene with Friedel-Crafts Catalyst

Lixin Xu, Mujie Yang

Department of Polymer Science and Engineering, Key Laboratory of Macromolecular Synthesis and Functionalization, Ministry of Education, Zhejiang University, Hangzhou 310027, China

Received 17 January 2008; accepted 22 April 2009
DOI 10.1002/app.30741
Published online 16 July 2009 in Wiley InterScience (www.interscience.wiley.com).

ABSTRACT: The application of Friedel-Crafts (FC) alkylation reaction to the *in situ* compatibilization between polystyrene-grafted nano-sized TiO_2 (PS-grafted TiO_2) and polypropylene (PP) was assessed. The PS-grafted TiO_2 was first prepared via dispersion polymerization of styrene (St) using 3-(trimethoxysilyl) propyl methacrylate treated nano-sized TiO_2 (MPS-treated TiO_2) as cores, and then dispersed within PP by melt blending with different contents of FC catalyst, $AlCl_3$/St, to give PP/PS-grafted TiO_2 nanocomposites. The dispersion of PS-grafted TiO_2 in PP and interfacial adhesion of PP/PS-grafted TiO_2 nanocomposites were characterized by transmission electron microscopy (TEM) and scanning electron microscopy (SEM), respectively. The results indicated that the dispersion of PS-grafted TiO_2 in PP could be improved, with an enhancement of interfacial adhesion between TiO_2 and PP, by introducing FC catalyst with adequate concentration, which led to a better thermal stability and resistance to ultraviolet (UV) aging of PP/PS-grafted TiO_2 nanocomposites. The effect of FC catalyst on the compatibilization between the PS-grafted TiO_2 and PP was discussed based on FC alkylation reaction mechanism. © 2009 Wiley Periodicals, Inc. J Appl Polym Sci 114: 2755–2763, 2009

Key words: polystyrene-grafted nano-sized TiO_2; polypropylene; Friedel-Crafts catalyst; compatibilization; aging

INTRODUCTION

Nano-sized TiO_2 materials have attracted a great deal of attention owing to its versatility in optical, electrical, and photochemical properties.[1–8] As a strong UV absorber, nano-sized TiO_2 can improve the resistance to UV aging of polymers without shortcomings such as toxicity, short-life, etc. compared with organic UV absorbers.[9,10] However, the raw TiO_2 nanoparticles aggregate easily when dispersed in polymer matrix, such as PP, by melt blending process because of higher viscosity of matrix and poor compatibility between TiO_2 nanoparticles and polymer matrix.[11] The existence of TiO_2 agglomerates reduces greatly the interfacial area between nanopartilces and polymer matrix, which results in a poor resistance to UV aging of polymers.[12]

Many methods have been explored to prepare the polymer nanocomposites, such as surface modification of nanoparticles with coupling agent,[13,14] sol–gel blending technique,[15] *in situ* polymerization process,[16–18] *in situ* forming nanoparticles route,[19] and polymer grafting from the surface of nanoparticles,[20–22] etc. Among them, the grafting of polymers from the surface of nanoparticles is becoming an important method because the prepared polymer-gafted nanoparticles offer very interesting actual and potential applications in many areas such as adhesives, textiles, optics, and electronics, etc.[23] In our previous work, a better dispersion of PS-grafted TiO_2 in PP was obtained by melt blending compared with the raw TiO_2 nanoparticles. The PS chains at the surface of TiO_2 nanoparticles prevent nanoparticles from aggregating to a certain extent. However, the poor compatibility between PS and PP matrix resulted in a poor interfacial adhesion of PS-grafted TiO_2 particles and matrix, and restricted further improvement in dispersion of TiO_2 nanoparticles.

Among the reactive phase compatibilization methods, the low-cost Friedel-Crafts alkylation reaction is an attractive route to compatibilize thermoplastic blends that contain PS.[24] By this reaction, a hydrocarbon chain can be chemically bonded to the benzene ring of PS through an aromatic electrophilic substitution and the resulting graft copolymer, polyolefin-g-PS, will behave as *in situ* compatibilizer for

Correspondence to: M. Yang (yangmj@zju.edu.cn).
Contract grant sponsor: Innovation Foundation of Hangzhou Municipal Scientific Department; contract grant number: 20052431B09.

TABLE I
Compositions for All Samples Prepared

Samples	PP/g	Raw TiO_2/g	MPS-treated TiO_2/g	PS-grafted TiO_2/g	$AlCl_3$/g	St/g
Pure PP	100	–	–	–	–	–
PPT	98	2	–	–	–	–
PPTM	98	–	2	–	–	–
PPTPS 0.0	97.7	–	–	2	0.0	0.3
PPTPS 0.3	97.4	–	–	2	0.3	0.3
PPTPS 0.5	97.2	–	–	2	0.5	0.3
PPTPS 0.7	97.0	–	–	2	0.7	0.3
PPTPS 1.0	96.7	–	–	2	1.0	0.3

the specific polyolefin/PS blend.[25–27] Although much work has been conducted to compatibilize the PP/PS[24] or PE/PS[28–30] blends by FC alkylation reaction, few studies have been reported on the compatibilization between the PS-grafted TiO_2 and PP using FC catalyst. In the present work, the TiO_2 nanoparticles were first grafted with PS and then added in PP with FC catalyst by melt blending. It is expected that the dispersion of the PS-grafted TiO_2 in PP and interfacial adhesion of PP/PS-grafted TiO_2 nanocomposites could be improved by means of *in situ* compatibilization between the PS-grafted TiO_2 and PP matrix.

EXPERIMENTS

Materials

Nano-sized TiO_2, which has the average particle size of 50 nm and mainly composed of rutile phase, was purchased from Zhejiang Zhoushan Mingri Nanomaterials Co. Ltd., China. Polypropyrene (PP) used in the present work is F401 from Sinopec Yangzi Petrochemical Co. Ltd., China, with a melt flow index (MFI) of 2.3 g/10 min at 230°C. The monomer, styrene(St), was purified on distillation under reduced pressure and the initiator, 2,2′-azobis (isobutyronitrile) (AIBN), was recrystallized from absolute ethanol and dried in vacuum before use. The silane coupling agent, 3-(trimethoxysilyl) propyl methacrylate (MPS), was purchased from Acros organics and used as received. Other reagents were all analytical grade.

Preparation of the PS-grafted TiO_2

The PS-grafted TiO_2 was prepared via St dispersion polymerization in the presence of MPS-treated TiO_2 particles. In a typical procedure, 4.0 g of nano-sized TiO_2 dried at 120°C for 10 h was added in 400 mL of absolute ethanol containing 4 g of MPS and 0.2 g of deionized water. The mixture was ultrasonicated at room temperature for 30 min to form a homogeneous suspension and then was refluxed at 80°C for 6 h under vigorous stirring with pH value at 4–5 adjusted by acetic acid. The resulted suspension was centrifugated at 16,000 rpm for 15 min, the precipitate obtained was redispersed in 30 mL of fresh absolute ethanol and centrifuged again. The cycle of "dispersion-centrifugation" was repeated at least 5 times to remove the unreacted MPS. The resulted powder was dried at room temperature overnight in vacuum, giving the MPS-treated TiO_2. The resulted MPS-treated TiO_2 (3.0 g) was dispersed in 300 mL of isopropanol by ultrasonication and 10.0 g of St containing AIBN (0.20 g) was added subsequently. The polymerization was performed under nitrogen atmosphere at 80°C for 24 h. The suspension was centrifuged at 16,000 rpm for 10 min, the precipitate was redispersed in toluene and centrifuged. The cycle of "dispersion-centrifugation" was repeated for 5 times to remove the free PS from the samples, the resulted powder was dried in vacuum at 45°C for 24 h, giving the purified PS-grafted TiO_2.

In situ compatibilization

The prepared PS-grafted TiO_2 was dispersed within PP by melt blending process with different contents of FC catalyst, $AlCl_3$/St, to prepare a series of PP/PS-grafted TiO_2 nanocomposites (PPTPS 0.0–1.0). The blending procedue includes the initial melting of PP matrix, and subsequent incorporation of TiO_2 powders along with FC catalyst. The blending was performed in a batch mixer at 200°C, 60 rpm for 25 min and then the obtained nanocomposites were pressed at 190°C, 15 MPa for 5 min to give sheets with a thickness of 1 mm used for measurements. For the sake of comparison, the pure PP, PP/MPS-treated TiO_2 (PPTM) and PP/raw TiO_2 (PPT) composites without FC catalyst were also prepared according to the same procedure. Table I shows the compositions of all samples prepared.

Measurements

The Fourier-transform infrared (FT-IR) spectra of nano-sized TiO_2 before and after treatment was recorded using a BRUKER VECTOR-22 spectrometer

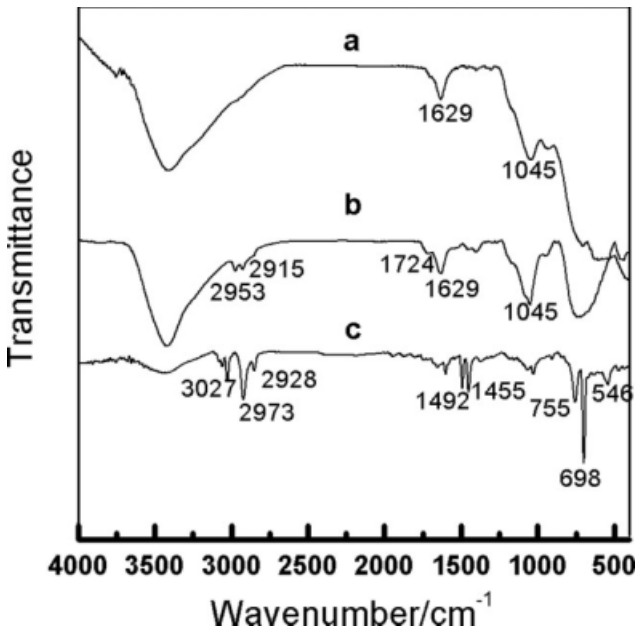

Figure 1 FT-IR spectra for the raw TiO_2 (a), MPS-treated TiO_2 (b), and PS-grafted TiO_2 (c).

over the range of 400–4000 cm^{-1} by averaging 128 scans at a maximum resolution of 2 cm^{-1}.

The contents of C, H, and N elemental in various TiO_2 samples were determined by elemental analysis (EA) using a Perkin-Elmer 2400 series analyzer. Thermogravimetry analysis (TGA) was performed on a Perkin-Elmer 7 series thermal analysis system at a heating rate of 20°C/min over a temperature of 50–650°C under nitrogen flow. The morphology of PS-grafted TiO_2 particles and its dispersion status in PP were observed by transmittance electron microscopy (TEM) using a JEM-100CXII electron microscopy at an accelerator voltage of 100 kv. For the nano-sized TiO_2 powder, the TEM specimens were prepared by dispersing the TiO_2 particles in absolute ethanol by ultrasonication and then depositing it on a 200-mesh copper grid. The block samples were cut on cryogenic conditions to give 50–70 μm thick section used for TEM analysis. The cross-sectional morphology of PP/PS-grafted TiO_2 nanocomposites were investigated by scanning electron microscopy using XL30-ESEM system. Samples were fractured at cryogenic temperature and then coated with Au in a PELCO 91,000 sputter coater used for SEM analysis. The X-ray photoelectron spectroscopy (XPS) of nano-sized TiO_2 before and after treatment was recorded on a ESCALAB 250 spectrometer using Mg Kα radiation. Specimens were analyzed at an electron take-off angle of 45° with respect to the surface plane. General survey scans (binding energy range: 0–1100 eV, pass energy: 70.0 eV) and high-resolution spectra (pass energy: 20.0 eV) in the regions of C1s, T2p, O1s were recorded for all samples. The UV artificially accelerating aging test was performed to compare the resistance to UV aging of various PP nanocomposites. The aging was performed at 60°C for 15 days in an UV accelerometer (Z-UV, china) using eight fluorescent bulb (UVB-313, 3.2 kw) with irradiance at 280–400 nm. Tensile strength of samples artificially weathered for 15 days were measured using an electron tensile apparatus (CMT5104, China) at a drawing rate of 50 mm/min. Dogbone tensile specimens with dimension of 80 × 5 × 1.0 mm were cut from the sheets prepared by compression molding mentioned earlier.

RESULTS AND DISCUSSION

FT-IR measurements

The grafting of PS from the surface of nano-sized TiO_2 was verified in the FT-IR spectra shown in Figure 1. In the spectrum of the raw nano-sized TiO_2 [Fig. 1(a)], the peaks at around 3300 cm^{-1} and 1629 cm^{-1} originate from the adsorbed water at the surface of TiO_2 particles.[31,32] After the modification with coupling agent, MPS, the absorption peaks characteristic of MPS appeared in the spectrum of the MPS-treated TiO_2 [Fig. 1(b)]. The peak at 1724 cm^{-1} is assigned to the stretching vibration of C=O groups and the peak near 2953 cm^{-1} caused by the C—H asymmetric stretching vibration of the methyl group in MPS molecules. The peak of C=C at 1629 cm^{-1} could not be detected separately probably due to the overlapping with the strong peak of adsorbed water in the same frequency region.[33] These indicated that the MPS has been grafted to the surface of TiO_2 particles. In the spectrum [Fig. 1(c)] of the purified PS-grafted TiO_2, from which the free PS has been removed completely, the characteristic absorption peaks of PS could be found at 3027 cm^{-1}, 1492

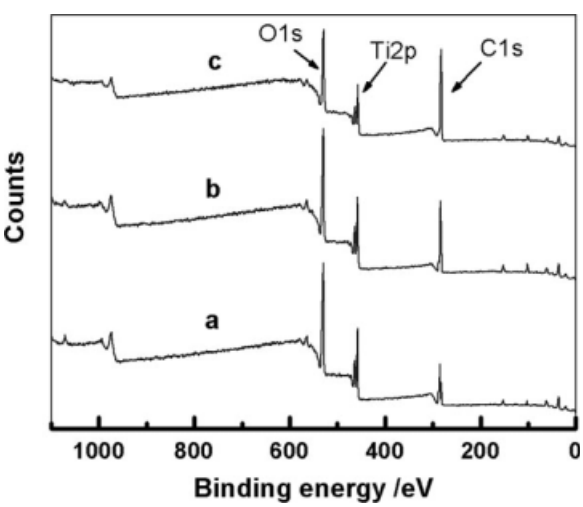

Figure 2 XPS wide scan spectra for the raw TiO_2 (a), MPS-treated TiO_2 (b), and PS-grafted TiO_2 (c).

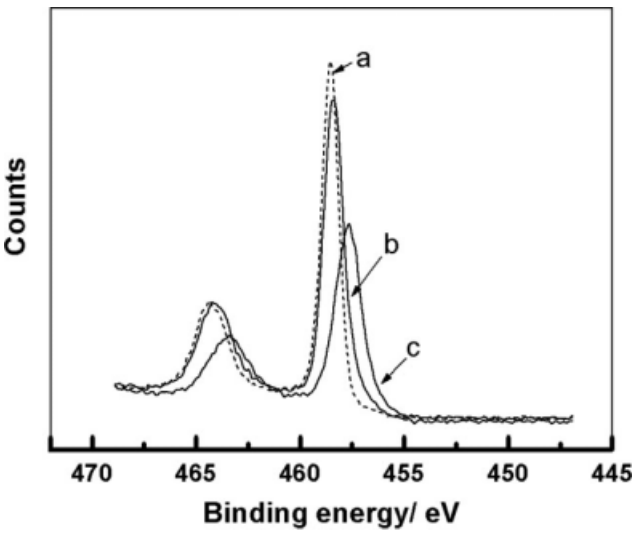

Figure 3 The XPS narrow scan spectra of Ti2p for the raw TiO_2 (a), MPS-treated TiO_2 (b), and PS-grafted TiO_2 (c).

cm^{-1}, 1455 cm^{-1}, 755 cm^{-1}, 698 cm^{-1}, 546 cm^{-1}, indicating that PS has been chemically bonded to the surface of nano-sized TiO_2.

XPS analysis

Figure 2 shows the XPS wide scan spectra of nano-sized TiO_2 before and after surface modification. The raw TiO_2 is mainly composed of elmental Ti and O as shown in Figure 2(a). The photoelectron peak of Ti2p appears at 458 eV, with O1s at 531 eV. However, the peak of C1s at 285 eV was also found in the spectrum of the raw TiO_2. This can be attributed to the existence of residual carbon or contamination at the surface of TiO_2 particles. For the MPS-treated TiO_2, the amount of elemental C increased obviously [Fig. 2(b)] compared with the raw sample, due to the introduction of coupling agent, MPS. After the grafting of PS from the surface of TiO_2 particles, the amount of C elemental was further enhanced, whereas that of Ti and O elemental decreased obviously [Fig. 2(c)] compared with both the the raw TiO_2 and the MPS-treated TiO_2. Moreover, the binding energy of Ti2p in the PS-grafted TiO_2 decreased slightly as shown in Figure 3. These indicate that the PS has been chemically bonded to the surface of nano-sized TiO_2 particles.

TABLE II
Elemental Analysis of the Raw TiO_2, MPS-Treated TiO_2, and PS-Grafted TiO_2

Sample	C/wt %	H/wt %	N/wt %
Raw TiO_2	0.977	0.977	0.075
MPS-treated TiO_2	3.033	1.041	0.184
PS-grafted TiO_2	10.667	1.578	0.170

Elemental analysis

The elemental analysis (EA) was performed to determine the contents of elemental C, H, and N in the nano-sized TiO_2 before and after surface modification and the results are presented in Table II. It could be found that the content of both C and H in the MPS-treated TiO_2 increase, compared with the raw sample, due to the introduction of MPS, and increased further after the grafting of PS from the surface of nano-sized TiO_2 particles. Here, we define the "grafting ratio" (*GR*) of PS as the mass percentage of PS relative to PS-grafted TiO_2. By calculating the data listed in Table II, the *GR* of PS for the PS-grafted TiO_2 is determined to be about 8.50 wt %.

SEM and TEM micrographs

The morphology of PS-grafted TiO_2 particles, before and after purification, was characterized by using TEM. Figure 4(a) shows the morphology of

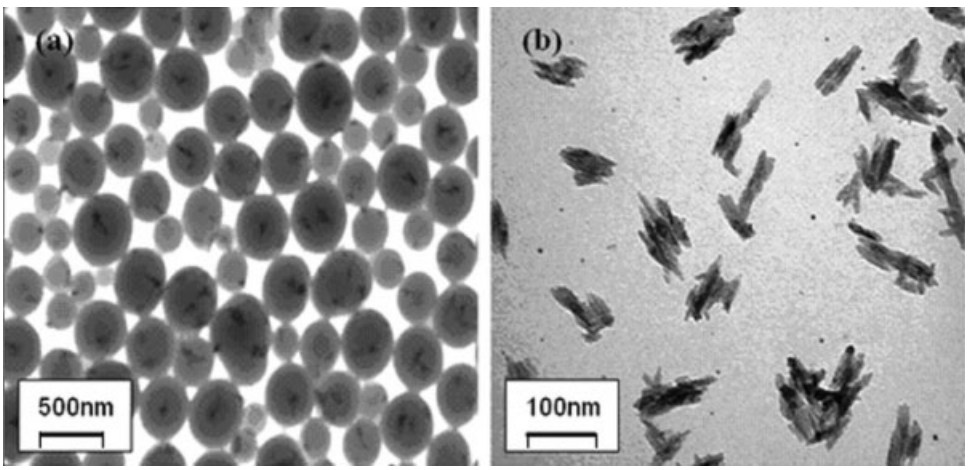

Figure 4 TEM micrographs for the unpurified PS-grafted TiO_2 (a) and purified PS-grafted TiO_2 (b).

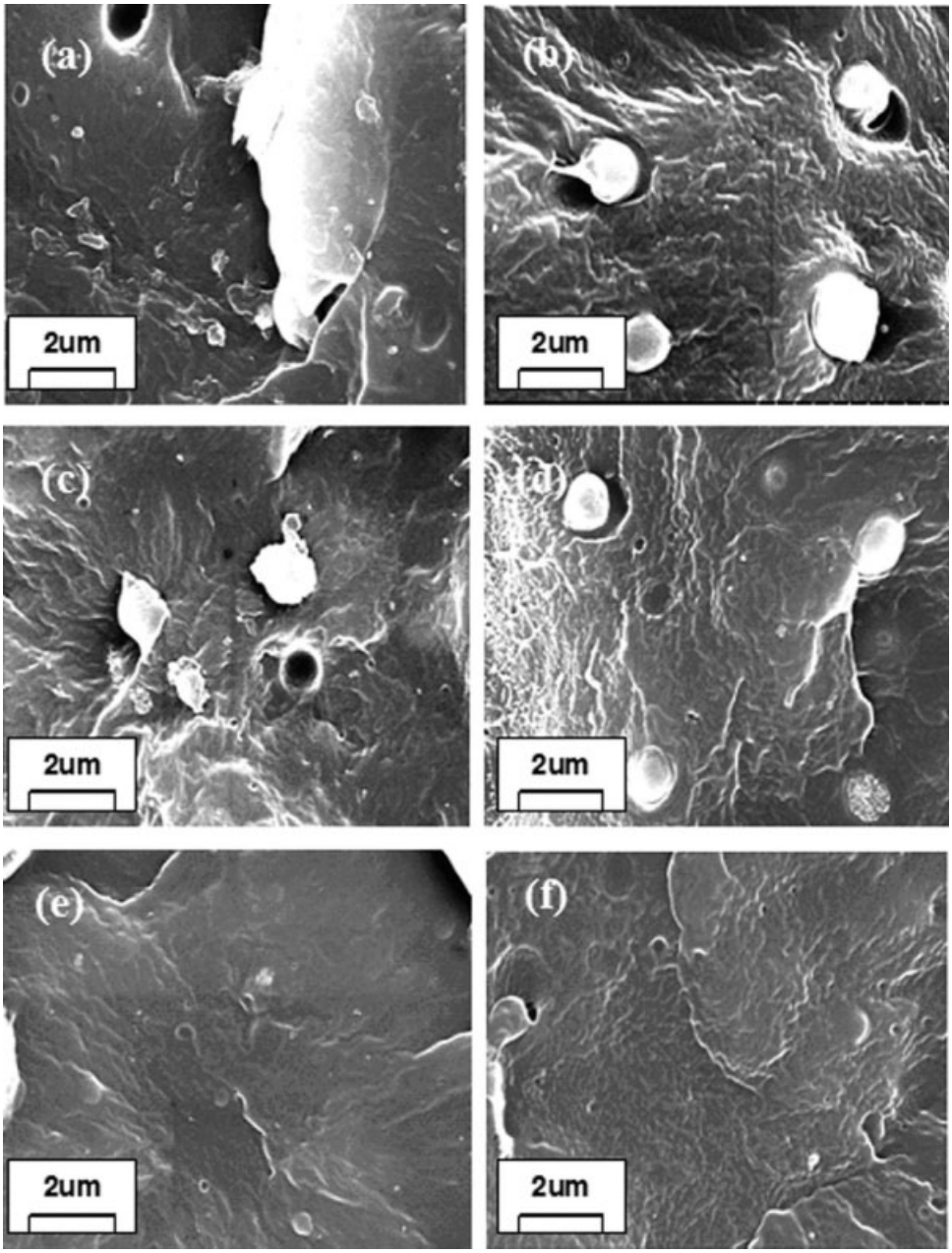

Figure 5 SEM micrographs for PPTM (a), PPTPS 0.0 (b), PPTPS 0.1 (c), PPTPS 0.3 (d), PPTPS 0.5 (e), and PPTPS 1.0 (f).

unpurified PS-grafted TiO_2 particles. It can be shown that the unpurified particles display approximately spheric structure with a diameter size from 250 to 500 nm. The central black spot and translucent parts in the composite particles show TiO_2 nanoparticles and PS polymer, respectively. It can be clearly found that TiO_2 nanoparticles were encapsulated into the polymer phase and appeared to be monodisperse in size approximately 100–120 nm length range. The morphology of purified PS-grafted TiO_2 particles is shown in Figure 4(b). A great difference can be found by comparing the morphology of composite particles before and after purification. The approximately spheric structure was destroyed by removing the free PS from composite particles. The translucent part in the purified composite particles shows the PS polymer layer, which coats on the surface of TiO_2 nanoparticles as grafting polymer. The grafting of PS from the surface of TiO_2 nanoparticles was testified by above results.

To examine the effect of FC catalyst on the dispersion of PS-grafted TiO_2 particles in PP matrix, we prepared a series of PP/PS-grafted TiO_2 (PPTPS) nanocomposites by adding the purified PS-grafted TiO_2 in PP with different contents of FC catalyst. Figure 5 shows SEM micrographs of the fractured surfaces corresponding to PPTPS 0.0–1.0 samples. The micrograph of PP/MPS-treated TiO_2 (PPTM)

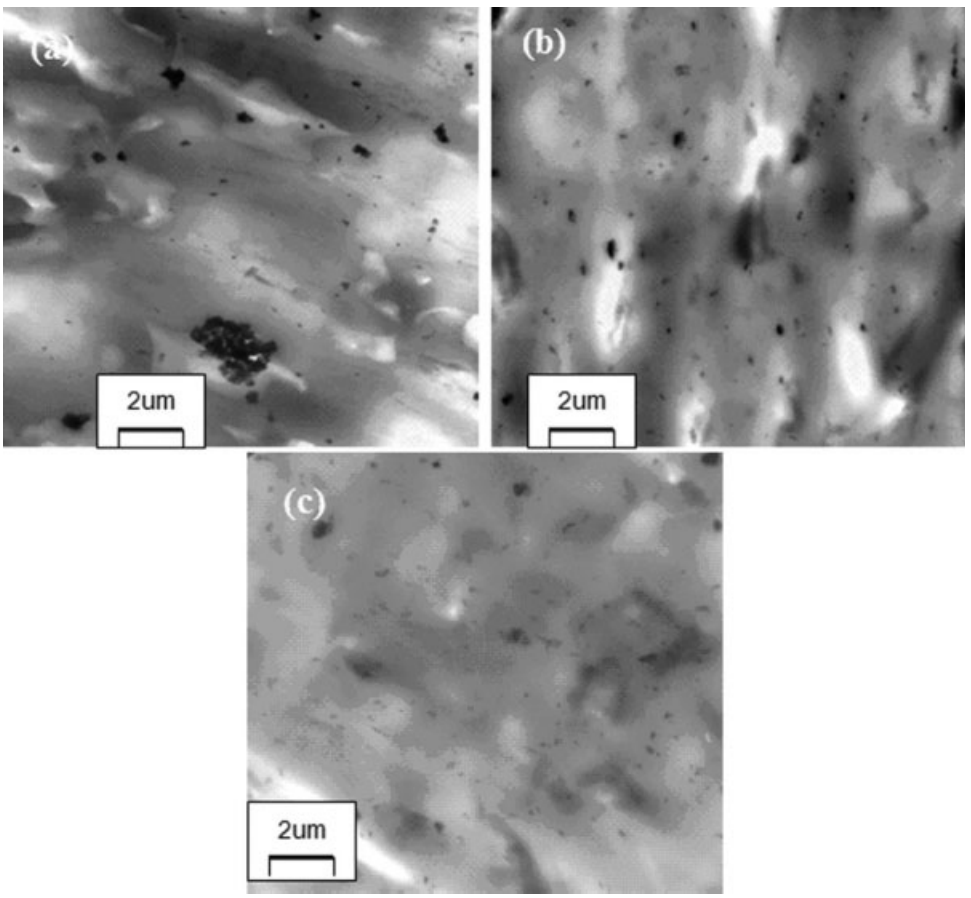

Figure 6 TEM micrographs for PPTM (a), PPTPS0.0 (b), and PPTPS 1.0 (c).

nanocomposite is also shown in Figure 5 for comparison. For the PPTM sample, the aggregation of TiO_2 nanoparticles larger than 0.5 μm is clearly observed, along with clear cavities left in PP matrix [Fig. 5(a)], indicating a bad dispersion and very weak adhesion. It has been reported that coupling agent, MPS, is usually grafted to the surface of TiO_2 nanoparticles under the form of oligomers rather than monomers owing to the presence of water in medium. Consequently, TiO_2 nanoparticles are difficult to be coated completely with MPS due to the steric hindrance of MPS oligomers, which led to a very bad dispersion of MPS-treated TiO_2 particles in PP and very weak adhesion as well. For the PPTPS series, as the FC catalyst content increased, a consistent improvement in adhesion is clearly observed along with particles size decreasing [Fig. 5(b–f)]. It also appears that for catalyst concentration reaches 1.0 wt %, the interphase becomes almost undiscernibly, indicating very good adhesion.

Figure 6 shows TEM micrographs of the PPTM, PPTPS 0.0, and PPTPS 1.0 samples. The black spots are TiO_2 nanoparticles. The grafting PS phase was merged with PP matrix, so only the morphology of TiO_2 nanoparticles could be observed. For the PPTPS 1.0 sample, the PS-grafted TiO_2 appeared to be monodispersed in PP matrix in size range of 100–150 nm [Fig. 6(c)]. The dispersibility of the composite particles in PP was improved greatly by adding 1.0 wt % of FC catalyst, compared with both PPTM [Fig. 6(a)] and PPTPS 0.0 sample [Fig. 6(b)].

UV artificially accelerating aging test

The UV artificially accelerating aging tests were performed to evaluate the resistance to UV aging of various PP samples. The tensile strength of all samples was measured before and after aging. The percentage of tensile strength of each sample weathered for 15 days relative to that before aging was simplified as "PT" and shown in Table III. The "PT" of pure PP is only 45.3%, showing a very bad resistance to UV aging. The PT increased, from 45.3 to 55.1%, when 2 wt % of raw nano-sized TiO_2 was added. This shows the UV-shielding effect of nano-sized TiO_2, which results from a quantum effect of the nanoparticles when the size of particles is reduced to a nanoscale.[34] Only a slight increment in PT, from 55.1% (PPT) to 57.0% (PPTM), was found when the TiO_2 nanoparticles were surface modified with MPS. However, the PT increased obviously, from 57.0 to 73.2%, when the PS-grafted TiO_2 was

TABLE III
Retention Percentage of Tensile Strength for Various Samples Artificially Weathered

Sample	PT[a]/%
Pure PP	45.3
PPT	55.1
PPTM	57.0
PPTPS 0.0	73.2
PPTPS 0.7	80.1
PPTPS 1.0	87.6

[a] Percentage of the tensile strength for the samples artificially weathered for 15 days relative to that before aging.

added and was further enhanced by introducing FC catalyst. The PT of PPTPS 0.7 and PPTPS 1.0 sample is 80.1 and 87.6%, respectively. This shows that the weatherability of PP filled with TiO_2 nanoparticles could be improved markedly by grafting of PS from the surface of nanoparticles and introducing FC catalyst with adequate concentration, which may be attributed to the improvement in dispersion of TiO_2 nanoparticles in the matrix.

Thermal analysis

The TGA curves of pure PP, PPT, and PPTPS 1.0 sample are shown in Figure 7. It can be seen that all samples exhibit a one-step weight loss both in the TG curves [Fig. 7(a)] and DTG curves [Fig. 7(b)]. This indicates that the degradation of all samples can be regarded as one-step degradatoin. The pure PP shows a onset decomposition temperature (T_{onset}) of 263.5°C, with a peak decomposition temperature (T_{peak}) corresponding to the maximum weight loss rate of 445.7°C. The T_{onset} and T_{peak} of PPT, which contains 2.0 wt % of raw TiO_2 nanoparticles, is 263.7 and 449.9°C, respectively, indicating that only a slight improvement in thermal stability was obtained compared with the pure PP. When the purified PS-grafted TiO_2 was added in PP with FC catalyst, the T_{onset} and T_{peak} of PPTPS 1.0 sample are shifted to a higher temperature range (434.5 and 476.3°C, respectively) compared with that of both pure PP and PPT sample, showing a greatly improved thermal stability of the composite. Such an improvement in thermal stability may be attributed to the stronger interfacial adhesion between the PS-grafted TiO_2 particles and PP matrix, which reduced the mobility of PP chains and thus slow the degradation process.[35]

DISCUSSION

The grafting of PS from the surface of nano-sized TiO_2 particles was confirmed by the results from FT-IR, XPS, EA, and TEM. The synthesis mechanism is shown in Scheme 1. The methoxy group of MPS first hydrolyze owing to the presence of water in the medium and subsequently associate to form oligomers. These oligomers were adsorbed on the surface of TiO_2 particles by hydrogen bonding and subsequently grafted to the surface of TiO_2 particles by condensation. Then St monomer can radical copolymerize with the double bond in the grafted MPS molecules to give chemically bonded PS chains on the surface of TiO_2 particles.

An improvement in the dispersion of PS-grafted TiO_2 particles in PP, along with an enhancement of adhesion between TiO_2 nanoparticles and PP matrix, was achieved by introducing FC catalyst with adequate concentration. This may be attributed to the *in situ* compatibilization between the PS, bonded chemically on the surface of TiO_2 particles, and PP matrix by FC alkylation reaction, which previously proposed to compatibilize PS/PE,[28–30] or PS/PP[24,25] blends in many studies. A general mechanism of this reaction was proposed in previous studies,[28–30] in which a low-molecular-weight carbocation is first formed. Then the carbocation yields a macrocarbocation by hiting the PE or PP molecules. Finally, the macrocarbocation produced a graft copolymer, PP-g-

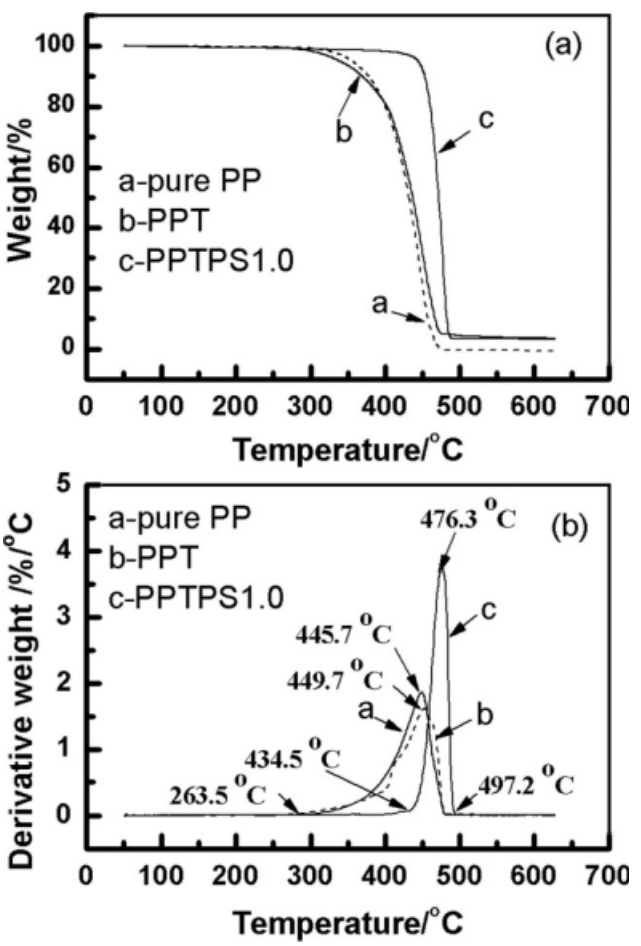

Figure 7 TG (a) and DTG (b) curves for the pure PP, PPT, and PPTPS 1.0 samples.

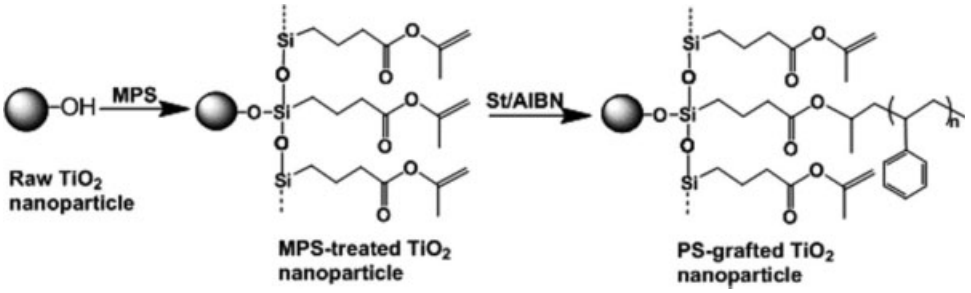

Scheme 1 Synthesis of PS-grafted TiO_2 through St dispersion polymerization.

PS or PE-g-PS, as compatibilizer by electrophilic attack on the PS benzene ring. Here, a similar mechanism is expected on the *in situ* compatibilization between the PS-grafted TiO_2 and PP based on previous studies (Scheme 2).[30] The aluminum chloride first reacts with water as impurity to form a complex, which subsequently further reacts with unsaturated compound, St as cocatalyst, forming the initial carbocation. The initial carbocation attacks PP chains to form a PP macrocarbocation, which finally substitutes for a proton from the benzene ring of PS on the surface of TiO_2 particles, forming a copolymer, PS-g-PP as compatibilizer between the TiO_2 particles and PP matrix. The direct evidence was not presented here for the difficulties in characterization of PS-g-PP copolymer, bonded chemically on the surface of TiO_2 nanoparticles, by regular methods. The further study is now in progress.

CONCLUSIONS

The PS-grafted TiO_2 has been synthesized by dispersion polymerization of St using the MPS-treated TiO_2 particles as cores. The TiO_2 particles were encapsulated into PS phase in size of 100–120 nm and the grafting ratio of PS is about 8.5 wt %. The dispersion of PS-grafted TiO_2 particles in PP could be improved greatly, with an enhanced interfacial adhesion between PS-grafted TiO_2 particles and PP matrix, by introducing FC catalyst with adequate concentration, which led to a better thermal stability and resistance to UV aging of PP/PS-grafted TiO_2 nanocomposites. The *in situ* compatibilization between the PS-grafted TiO_2 particles and PP may be attributed to the FC alkylation reaction, which holds potential application in the preparation of PP nanocomposites with high performance.

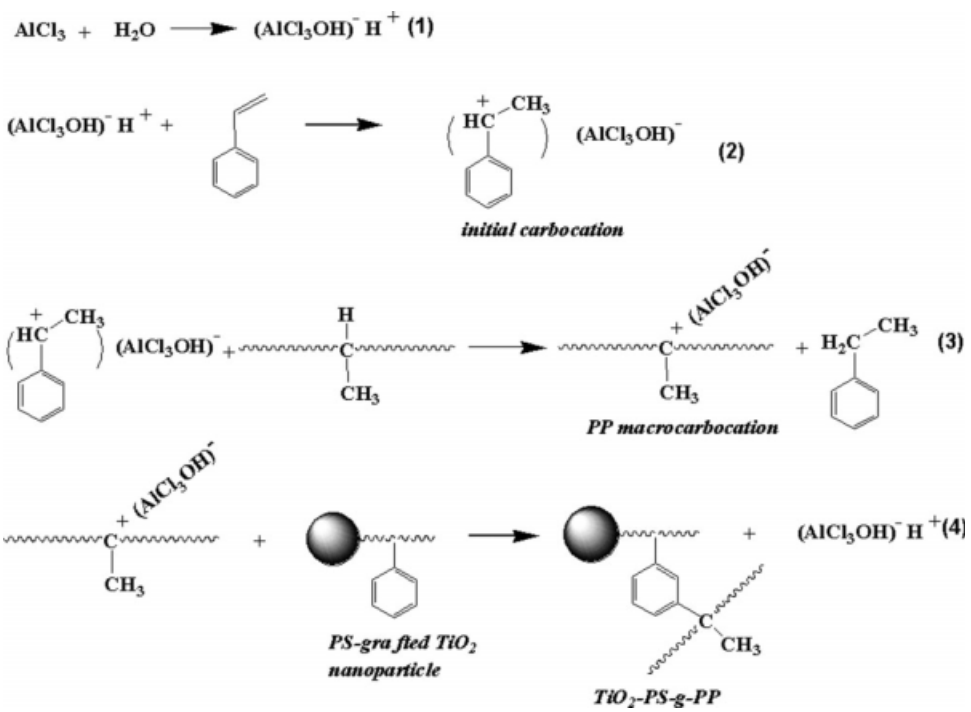

Scheme 2 *In situ* compatibilization between the PS-grafted TiO_2 particles and PP by FC alkylation reaction.

References

1. Vogel, R.; Mererdith, P.; Kartina, I.; Harvey, M.; Riches, J. D.; Bishop, A.; Heckenburg, N.; Trau, M.; Rubinsztein-Dunlop, H. Chem Phys Chem 2003, 4, 595.
2. Boschloo, G.; Hagfeldt, A. Chem Phys Lett 2003, 370, 381.
3. Francioso, L.; Presicce, D. S.; Taurino, A. M.; Rella, R.; Siciliano, P.; Ficarella, A. Sensor Acuate B- Chem 2003, 95, 66.
4. Du, X. Y.; Wang, Y.; Mu, Y. Y.; Gui, L. L.; Wang, P.; Tang, Y. Q. Chem Mater 2002, 14, 3953.
5. Hansel, H.; Zettl, H.; Krausch, G.; Kisselev, R.; Thelakkat, M.; Schmidt, H. W. Adv Mater 2003, 15, 2056.
6. Kron, G.; Rau, U.; Werner, J. H. J Phys Chem B 2003, 107, 13258.
7. Bosc, F.; Ayral, A.; Albouy, P. A.; Guizard, G. Chem Mater 2003, 15, 2463.
8. Nakamura, R.; Imanishi, A.; Murkoshi, K.; Nakato, Y. J Am Chem Soc 2003, 125, 7443.
9. Zhang, Y.; Zhou, G. E.; Zhang, Y. H.; Li, L.; Yao, L. Z.; Mo, C. M. Mater Res Bull 1999, 5, 701.
10. Sung, Y.-M.; Yung-Soo, P. K.; Sang, M. P.; Gopinathan, M. J Cryst Growth 2006, 286, 173.
11. Acierno, D.; Filippone, G.; Romeo, G.; Russo, P. Macromol Symp 2007, 247, 59.
12. Keqing, H.; Han, Y. J Appl Polym Sci 2006, 100, 1588.
13. Tee, D. I.; Mariatti, M.; Azizan, A.; See, C. H.; Chong, K. F. Compos Sci Technol 2007, 67, 2584.
14. Zou, W. J.; Peng, J.; Yang, Y.; Zhang, L. Q.; Liao, B.; Xiao, F. R. Mater Lett 2007, 61, 725.
15. Juangvanich, N.; Manritz, K. A. J Appl Polym Sci 1998, 67, 1799.
16. Lantelme, B.; Dumon, M.; Mai, C.; Pascanlt, J. P. J Non-Cryst Solids 1996, 194, 63.
17. Li, Y.; Yu, J.; Guo, Z.. Polym Int 2003, 52, 981.
18. Chang, J.; Kim, S. Polymer 2004, 45, 919.
19. Shen, L.; Du, Q.; Wang, H.; Zhong, W.; Yang, Y. Polym Int 2004, 53, 1153.
20. Bartholome, C.; Beyou, E.; Bourgeat-Lami, E.; Cassaganau, P.; Chaumont, P.; David, L.; Zydowicz, N. Polymer 2005, 46, 9965.
21. Luna-Xavier, J.; Guyot, A.; Bourgeat-Lami, E. J Colloid Interface Sci 2002, 250, 82.
22. Bartholome, C.; Beyou, E.; Bourgeat-Lami, E.; Chaumont, P.; Zydowicz, N. Macromolecules 2003, 36, 7946.
23. Bourgeat-Lami, E.; Jacques, L. J Colloid Interface Sci 1998, 197, 293.
24. Monica, F. D.; Silvia, E. B.; Numa, J. C. Polymer 2005, 46, 6096.
25. Diaz, M.; Barbosa, S.; Capiati, N. Polymer 2002, 43, 4851.
26. Diaz, M.; Barbosa, S.; Capiati, N. J Polym Phys 2004, 42, 452.
27. D'orazia, L.; Guarino, R.; Mancarella, C.; Martuscelli, E.; Cecchin, G. J Appl Polym Sci 1997, 65, 1539.
28. Carrick, W. L. J Polym Sci Polym Chem Ed 1970, 8, 215.
29. Sun, Y.; Willemse, R.; Liu, T.; Baker, W. Polymer 1998, 39, 2201.
30. Sun, Y.; Baker, W. J Appl Polym Sci 1997, 65, 1385.
31. Deng, C.; James, P. F.; Wright, P. V. J Mater Chem 1998, 8, 153.
32. Park, H. K.; Kim, D. K.; Hee, C. J Am Cerama Soc 1997, 80, 743.
33. Siddiquey, I. A.; Ukaji, E.; Furusawa, T.; Sato, M.; Suzuki, N. Mater Chem Phys 2007, 105, 162.
34. Nyffenegger, R. M.; Craft, B.; Shaaban, M.; Gorer, S.; Erley, G.; Penner, R. M. Chem Mater 1998, 4, 1120.
35. Tang, E. J.; Liu, H.; Sun, L. M.; Zheng, E. L.; Cheng, G. X. Eur Polym J 2007, 10, 4210.